Thermally treated peanut oil bodies as a fat replacer for ice cream: Physicochemical and rheological properties

Farah ZAABOUL[1,2]*, Tian TIAN[1], Pallab Kumar BORAH[2], Vincenzo DI BARI[2*]

[1]*State Key Laboratory of Food Science and Technology, School of Food Science and Technology, National Engineering Research Center for Functional Food, National Engineering Laboratory for Cereal Fermentation Technology, Collaborative Innovation Center of Food Safety and Quality Control, Jiangnan University, 1800 Lihu Road, Wuxi, Jiangsu 214122, China*

[2]*Food and Biomaterials Group, School of Biosciences, University of Nottingham, LE12 5RD, United Kingdom*

*Corresponding author: farahzaaboul@jiangnan.edu.cn; Farah.Zaaboul@nottingham.ac.uk

Co-corresponding author: Vincenzo.dibari@nottingham.ac.uk

16 **Graphical abstract**

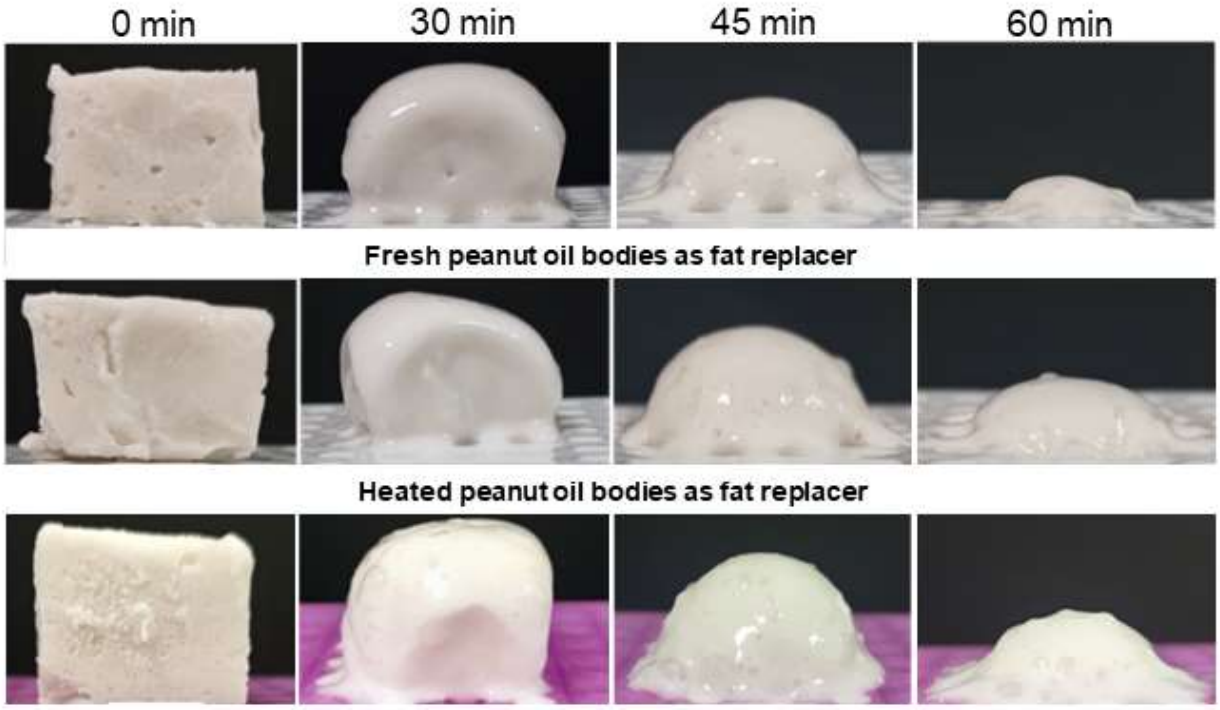

17

18

Abstract:

This study investigates the potential use of peanut oil bodies as a fat replacer in ice cream. The research explores the effects of different treatments fresh (FOB), heated (HOB), and roasted (ROB) of peanut oil bodies on ice cream preparation. The heat treatment is found to alter the protein profile on the oil bodies' surface, subsequently influencing the ice cream's properties. Notably, heat treatment increases the oil bodies' size and the absolute value of zeta potential. The elastic modulus analysis provides information about void volumes, indicating easier air incorporation during whipping for ROB (72 to 300 nm) compared to FOB (107 to 55 nm). ROB ice cream displays a high overrun and a lower melting rate compared to FOB ice cream. Moreover, thermal treatment contributes to reducing the beany flavors, n-hexanal, and 2-pentenylfuran. Overall, this study reveals peanut oil bodies as a promising platform for designing fat-substituted plant-based ice creams.

Keyword: Ice cream; Peanut oil bodies; Proteins; Rheology; Overrun; Melting

1. Introduction:

Ice cream is a complex colloidal frozen system composed of partially coalesced fat droplets, air cells, ice crystals, and a continuous aqueous phase in which carbohydrates, proteins, and mineral salts are dispersed (Marshall, Goff, Hartel, Marshall, Goff, & Hartel, 2003). Typically, conventional ice cream formulations consist of a high fat content, ca. 10 – 16 % from dairy or non-dairy sources. Whilst fat an important ingredient in ice cream that affects its dryness, post-freezing shape retention, melt resistance, and smoothness after hardening, however when ice cream is frozen, the fat emulsion in the mixture is destabilized by whipping and ice crystallization. Here, the destabilized fat acts as a cementing agent and provides support for air bubbles, which are primarily stabilised by proteins. Partially coalesced fat provides firmness and structure to ice cream; a phenomenon mostly observed with animal-based fat. In recent years, due to high increase of proven links between the high consumption of saturated animal-based fat and cardiovascular diseases and obesity (Akalin & Karagzl), a need to eliminate or reduce fat in ice cream has gained tremendous scientific and industrial attention. This is a significant technological issue, as deleting or lowering the fat level of ice cream results in several inadequacies in product quality, ideal structural, functional, and sensory aspects. As a result, they cannot be readily substituted with liquid oils without affecting the organoleptic qualities of the product. A first-order solution to the challenge of replacing animal fats is to replace them with plant-based oils (Akbari, Eskandari, & Davoudi, 2019; Crizel, Araujo, Rios, Rech, & Flôres, 2014). However, such plant-based oils systems should be able to impart solid-like properties as long-chain fatty acids are known to be liquid, and it is a challenge to use them in the production of ice cream. In this regard, non-triglyceride structured oils (*i.e.* oleogelation) has shown considerable potential in recent years as a

unique technique to substitute animal-based fats in food items (Wang, Gravelle, Blake, & Marangoni, 2016).

In this regard, peanut oil bodies, which are lipid-storing organelles in peanuts have gained considerable attention in recent years (Zaaboul, Matabaro, Raza, Xin, Duhoranimana, Cao, et al., 2018). The purified peanut oil bodies consist mainly of neutral lipid droplets (ca. 98 %) surrounded by a monolayer of phospholipids and alkaline proteins, mainly oleosin (typically 16–24 kDa) and caleosin (typically 27–32 kDa) (Zaaboul, et al., 2018) besides extraneous proteins such as P34/Bd30, and lipoxygenase (Chen, Chen, Zhao, Kong, Yang, & Hua, 2018). It is the structure and topological orientation of such oil body intrinsic proteins, which make oil bodies useful as structured oils and tolerate stresses. Additionally, oils conserved in the peanut oil bodies do not differ from the oil extracted from the whole beans, with the dominant fatty acids being oleic acid (18:1), linoleic acid (18:2), palmitic acid (16:0), and stearic acid (18:0) (Zaaboul, Raza, Chen, & Liu, 2018). In addition, they contain high levels of vitamin E and phytosterols (Zaaboul, Raza, Chen, & Liu, 2018), which makes them highly suitable for use, in lieu of peanut oils obtained by conventional methods. In addition, peanut oil bodies have a creamy texture and can be diluted to form a natural oil-in-water emulsion, with high physico-chemical stability during processing (heat treatment, high-pressure homogenization, etc.) (Zaaboul, et al., 2018; Zaaboul, Raza, Cao, & Yuanfa, 2019; Sun, Wang, Gao, Xiao, & Yang, 2023). This is partly owing to surface proteins that ensure the higher integrity and stability of the oil bodies (Zaaboul, Zhao, Xu, & Liu, 2022; Sun, Wang, Gao, Xiao, & Yang, 2023). Since structured emulsions are known to aid in fat and oil reduction (Wang et al., 2016), peanut oil bodies have tremendous potential to be used as a plant-based fat replacer.

In this study, we explore plant oil bodies as a structured fat source for the preparation of ice cream with a high content of unsaturated fatty acids to improve the nutritional quality of ice cream, and as an alternative to animal-based fat. Here we tune the oil bodies via modification of the protein membrane, as oil body structure and stability are directly linked to their protein membrane. Taking advantage of protein's propensity to heat-induced modifications, we created oil bodies with varying protein profile to investigate the effect of protein membrane on the final product. We used three different samples of peanut oil bodies: oil bodies isolated from fresh peanuts (FOB), heated oil bodies (HOB), and oil bodies isolated from roasted peanuts (ROB). The lipid and protein profiles of the three samples are evaluated using complementary GC and UPLC along with Electrospray Ionization Quadrupole-Time-of-Flight Mass Spectrometry. The rheology, particle size, overrun and melting properties, microstructure, and volatiles of ice cream samples prepared from the three oil bodies are characterized to investigate the systems as novel fat source whilst maintaining ice cream quality. Additionally, the use of oil bodies in ice cream preparations eliminates the need for emulsification step during processing. This study provides the foundations for expanding the application of oil bodies in the food industry and developing healthy frozen foods.

2. Materials and Methods

2.1. Materials. The peanuts were purchased from the local market in Shandong Province, China. The peanuts were stored in sealing bag at 4°C until use. Sucrose was purchased from Beijing Sinopharm Group Chemical Reagent Co., Ltd. (Beijing, China) whey protein, was obtained from Shuangta Food Co., Ltd (Yantai, China), corn syrup was purched from local market and Food grade guar gum was purchasedfrom Deosen Biochemical Co., Ltd. (Zibo, China). All other reagents were purchased from Beijing Sinopharm Group Chemical Reagent Co., Ltd. (Beijing, China). Milli-Q water (18.2 MΩ.cm ionic purity at 25 °C) purified using a Milli-Q apparatus (Millipore Corp., USA) was used throughout the experiments.

2.2. Oil bodies preparation. Peanut oil bodies were isolated from fresh and roasted peanuts following the method described previously (Zaaboul, et al., 2018). Raw peanuts were roasted in a pilot-scale short-wave infrared roaster (Senttech Infrared Technology Co., Ltd, China) at 220°C for 15 min to obtain roasted peanuts. For oil body isolation, fresh and roasted peanuts were washed and soaked in water at 4°C for 6 h. The soaked peanuts were ground with water in a 1:9 ratio at 18,000 rpm for 2 min in a blender (MJ- 60BE01B, Midea, China). The blends were subjected to four grinding and filtering cycles to ensure that all oil bodies were released. The blends were then centrifuged at 25000g for 25 min, and the suspended top white cream was recovered and then washed twice as described previously (Zaaboul et al.). The oil body creams were collected and stored at 3°C for 12 hours before use (Zaaboul, et al., 2018). Oil bodies isolated from fresh and roasted peanuts are referred to as fresh oil bodies (FOB) and roasted oil bodies (ROB), respectively. Peanut oil bodies referred to in this manuscript are equivalent to fresh oil bodies (FOB). Additionally, FOB was suspended in water at 1:5 ratio and heated in a water bath at 85°C for 15 min. The heated sample was then allowed to cool to ambient temperatures and centrifuged

at 25000g for 25 min. The suspended top white cream was recovered and stored at 3°C for 12 hours before use and are referred to as heated oil bodies (HOB).

2.3. Physicochemical properties of oil bodies

2.3.1. Tricine SDS PAGE. Tricine SDS-PAGE of oil bodies was performed as described earlier (Zaaboul, et al., 2018). The gel was stained with Coomassie brilliant blue G-250 and the band intensities were analyzed using Image Lab software (Bio-Rad, Hercules, U.S.A.).

2.3.2. Fatty acid analysis. Total lipids were extracted from FOB, ROB, and HOB by homogenization with chloroform/methanol (2:1, v/v) as described earlier (Mao, Guo, Huang, Tang, Zhang, Yang, et al., 2022). The resulting oil was stored under nitrogen at - 20°C until analysis. Fatty acid analysis was determined by GC-2010 PLUS (SHIMADZU, Japan) after derivatization to FAMEs according to (Diaby, Amza, Onivogui, Zou, & Jin, 2016) with a slight modification. Briefly, 20 to 30 mg of oil sample was mixedwith 2 mL of methanolic NaOH incubated at 65°Ctoreactfor 30 min. The mixture was cooled down to room temperature,and then heated at 70°C for 10 min after adding 2 mL of themethanolic BF3solution. The excess water was removed by theaddition of sodium thiosulfate to the mixture and the FAME wasextracted with 2.0 mL of hexane followed by a slow centrifugationat 10000 rpm for 10 min. A supernatant of both oils was passedthrough a 0.45 mm membrane filter. A sample of 0.5 mL was injected to the GC. The flow rate of carrier gas was 1 mL/min. The oven temperature program was as follows: initial 60 °C for 3 min, raised to 175 °C at 5 °C/min, and held for 15 min, then increased to 220 °C at 2 °C/min and then held at 220 °C for 10 min. The injection volume of sample dissolved in hexane was 1 µL.

2.3.3. Triacylglycerol analysis. Triacylglycerols (TAGs) were identified as described earlier (Zaaboul, Cao, Raza, Jun, Xu, & Liu, 2019). Briefly, oils extracted from oil bodies were diluted in hexane to a final concentration of 10 mg mL^{-1}. TAGs were separated and identified using the Ultra-high performance liquid chromatography with quadrupole time-of-flight mass spectrometry using an ACQUITY UPLCBEH C18 analytical column (i.d. 2.1×50 mm, 1.9 mm). For an efficient separation of the lipids, two mobile phases were used forthe separation. Mobile phase A consisted of acetonitrile/water (4:6, v/v) while mobile phase B had acetonitrile/isopropyl alcohol (1:9, v/v).

2.3.4. Particle size distribution. The mean hydrodynamic diameter (D_h) and the surface charge of oil bodies were measured using dynamic light scattering on a Zetasizer Nano ZS (Malvern Instruments, UK) equipped with a 4 mW helium/neon laser at a wavelength output of 633 nm and backscattering was measured at a detection angle of 173°. During the measurements, the samples were diluted 10-times in water for analysis at 25 °C. Each value was measured at least three times.

2.4. Ice cream formulation. Ice-cream mix was prepared as described previously (Goff & Hartel, 2013; VanWees, Rankin, & Hartel, 2020). Briefly, 4% of whey protein was dissolved in water and allowed to fully hydrate for 12 hours at 4°C. A mix of 12% (w/w) of sucrose, 4% (w/w) of corn syrup, 0.5% (w/w) guar gum were dispersed in deionized water, separately. The hydrated solutions were mixture with continuous stirring at room temperature. Finally, 10% (w/w) oil bodies were added to the mix and blended at 13600 rpm for 200s using an Ultra-Turrax blender (T18, IKA, Staufen, Germany), and stored at 3°C for 24 h. After aging, the ice cream mix was whipped and frozen with an ice cream machine (constant temperature of −5 ◦C for 30 minutes), and the obtained ice cream was poured into plastic containers and hardened at -18◦C for 24 hours.

2.5. Ice cream material characterization

2.5.1. Rheological properties. Steady shear and oscillatory rheology of the ice cream mix samples were analyzed at 4°C on a DHR-3 rheometer with a Peltier temperature control system (TA Instruments, USA). A cone and plate geometry were used (diameter, d = 40 mm, angle, α = 4°; effective cone height, $h = tan\alpha\left({}^{d}/_{2}\right)$ = 1.39 mm). Measurements were carried out as frequency sweeps, within the linear viscoelastic range, at an amplitude of deformation (γ) = 1 % and angular frequency (ω) = 10^{-2} to 10^{2} rad s^{-1}. All samples were equilibrated for 3 min before starting the measurement. The sample zero-shear viscosity was derived from the plateau value of the complex viscosity, η^* using a Carreau-Yasuda fitting as, $\eta = \eta_\infty + (\eta_0 - \eta_\infty)\left[1 + \left(t\dot{\gamma}\right)^{a}\right]^{\frac{m-1}{a}}$, where η_0 is the zero shear viscosity (Pa·s). The consistency coefficient, K and flow behaviour, n was estimated by least-square fitting employing the Levenberg-Marquardt algorithm to a Power-Law equation as, $\eta^* = K\omega^{n-1}$. Elastic modulus, G', viscous modulus, G'' were recorded.

2.5.2 Overrun. The overrun of ice cream samples was measured as described previously (Bekiroglu, Goktas, Karaibrahim, Bozkurt, & Sagdic, 2022). Equal volumes of ice cream mixes before and after whipping were weighed to calculate ice cream overrun, as $Overrun(\%) = 100 \times {}^{(w_0 - w_1)}/_{w_1}$, where w_0 is the weight of the ice cream mix and w_1 the weight of ice cream mix after whipping.

2.5.3 Melting rate. The melting rate of ice cream samples were determined as described earlier (Wang, Li, Wang, Gu, Liu, Xu, et al., 2022) with some modifications. Briefly, the initial weight of the samples (at -18 °C) was measured and then placed over a mesh at ambient temperature (20 °C). Melt passing through the mesh was collected and the weight recorded to the last drop of each sample, and evaluated as,

180 $$Melting\ rate(\%) = 100 \times {}^{weight\ of\ melt}/_{weight\ of\ ice\ cream}$$

181 **2.5.4 Microscopy.** The morphology of the ice cream mix was visualized on Leica DM2700P
182 (Leica, Germany) equipped with a camera (Leica DFC450, Germany) using bright field while ice
183 cream was visualized using polarized light optics. The specimens were placed on glass slides,
184 covered with a coverslip, and immediately observed.

185 **2.5.5. Volatile analysis.** Volatile coumpounds in ice cream samples were separated using the
186 automatic headspace solid phase microextraction (HS-SPME) and analyzed using a GC-MS/MS
187 instrument (TSQ Quantum XLS, Thermo Fisher Scientific, USA). Four grams of mix samples was
188 added and sealed in 20 mL headspace vial. Volatile compounds were extracted by an automatic
189 head-space solid phase microextraction (HS-SPME) device equipped with the 50/30 µm
190 DVB/CAR/PDMS fiber. Before extraction, the fiber was pre-conditioned by inserting into the
191 injector port of the GC system and keeping at 270 °C for 2 h in the stream of helium and samples
192 were equilibrated at 60 °C for 15 min. After extraction, the SPME device was carried out in the
193 GC injector at 250 °C for 5 min in splitless mode. Components were identified by software
194 retrieval and matching against the NIST library database based on the principle that both the
195 forward search matching score (SI) and the reverse search matching score (RSI) are greater than
196 800.

197 **2.6. Statistical Analysis**. All results were expressed as mean values ± standard deviation. Data
198 were analyzed by analysis of variance (ANOVA), using Statistix 10 (Analytical Software, USA).
199 Treatment means were considered significantly different at $p < 0.05$.

200 **3. Results and Discussion**

First, we discuss the lipid and triglyceride composition alongside protein profile of the oil bodies isolated from fresh and roasted peanuts, viz., fresh oil bodies (FOB), heated oil bodies (HOB), and roasted oil bodies (ROB), as it sets the scene to understand the rheological, melting, and volatile aromatic composition of oil body incorporation into the ice-creams, as a fat replacer.

Table 1. Fatty acid and triacylglycerols composition of FOB, ROB, and HOB

Fatty acids (FAs)		FOB	ROB	HOB
		(%)	(%)	(%)
C16:0	Palmitic acid (P)	11.46 ± 0.09	11.9± 0.01	11.46± 0.03
C16:1	Palmitoleic acid (Pa)	0.02 ± 0.04	0.04± 0.01	0.02± 0.05
C18:0	Stearic acid (S)	4.03 ± 0.01	4.62± 0.08	4.33± 0.01
C18:1	Oleic acid (O)	42.42 ± 0.03	41.80± 0.02	41.42± 0.05
C18:2	Linoleic acid (L)	35.10 ± 0.07	32.34± 0.03	34.91± 0.05
C20:0	Arachidic acid (Ar)	1.77 ± 0.01	1.83± 0.01	1.78± 0.03
C18:3	Linolenic acid (Ln)	0.60 ± 0.06	0.76± 0.01	0.66± 0.05
C20:1	Paullinic acid (Pu)	0.68 ± 0.01	0.63± 0.04	0.62± 0.07
C22:0	Behenic acid	2.56 ± 0.02	2.22± 0.02	2.30± 0.02
C24:0	Lignoceric acid	1.32 ± 0.01	1.70± 0.01	1.32± 0.01
Total saturated FAs		21.14 ± 0.14[a]	22.27±0.13[a]	21.69± 0.14[a]
Total unsaturated FAs		78.82 ± 0.21[b]	75.57±0.11[b]	77.63± 0.21[b]

FOB: Fresh oil bodies. ROB: Roasted oil bodies, HOB: Heat treated oil bodies. Different letters within the same column are significantly different at $p < 0.05$

3.1 Lipid profile of Oil bodies. We first analyzed the lipid profile of the oil bodies as it plays an important role in the production of ice cream. The goal was to observe any differences in the lipid profile based on the processing conditions (heat treatment, *i.e.*, roasting and heating) and eventually relate the differences to the quality of the final product. The oils extracted from FOB, ROB and HOB were derived, and following this the methylated and fatty acid-methyl ester were quantified by gas chromatography. As observed from Table 1, we observed no difference in fatty acid composition or fatty acid percentages, indicating that heat treatment (roasting and heating)

did not affect the fatty acid profile of the oil bodies. The dominant fatty acids found in all samples were: oleic acid (18:1), linoleic acid (18:2), palmitic acid (16:0) and stearic acid (18:0); with an overall 4.5% long chain fatty acid composition. Our results are in good agreement with our previous work on peanut oil bodies, where we found no difference between the oil in oil bodies isolated under different conditions and the oil extracted from the whole beans. For example, in our previous study we found that the major fatty acids were oleic acid (18:1), linoleic acid (18:2), palmitic acid (16:0), stearic acid (18:0), and behenic acid (22:0) (Zaaboul, Raza, Chen, & Liu, 2018), and corroborates our present work. It is of note that vegetable oils are usually low in saturated fatty acids, which tends to make them a liquid even at low temperatures. However, peanut oil can begin to crystallize at 3°C due to its relatively high saturated fatty acid content compared with other vegetable oils such as soybram oil, sunflower oil, linseed oil, etc. For the peanut variety used in our work, the saturated fatty acid content was 21.44%, 22.70%, and 21.69% for the FOB, ROB, and HOB, respectively, which is also in good agreement with our previous work (Zaaboul, Raza, Chen, & Liu, 2018).

Additionally, Supplementary Table S1 shows 23 individual triacylglycerols (TAGs) separated from all samples. The elution order of TAGs was determined by their partition numbers (PN), where PN= (the carbon number (CN) - twice the number of double bonds). The retention time increases with the increase of PN and the TAGs with small carbon number eluted earlier. However, the TAGs with the same CN eluted according to the number of unsaturated bonds, and TAGs with fewer double bonds eluted first. As expected, it can be seen that the oils generally have the same TAG profile and all samples contain the same dominant TAGs represented in OOO, OOL, POO, POL and OLL. In general, these results agree with the results of previous studies on peanut oil, but with varying degree (Sempore & Bezard, 1986; Singleton & Pattee, 1987).

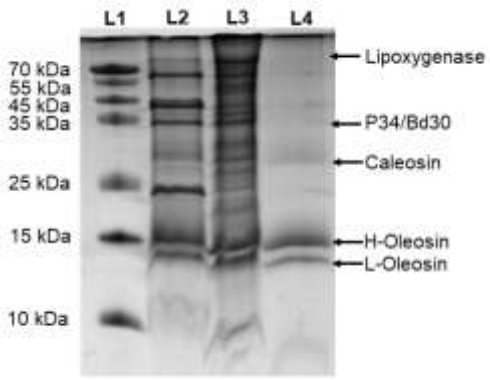

Figure 1. Tricine SDS-PAGE of oil bodies. Lanes indicate, L1, protein marker; L2, fresh oil bodies (FOB); L3, roasted oil bodies (ROB); L4, heated oil bodies (HOB). Arrows indicate proteins based on molecular weight.

As described earlier in the introduction, peanut oil bodies are surrounded by a monolayer comprising of phospholipids and alkaline proteins, and the structure and topological orientation of such oil body intrinsic proteins, make oil bodies useful as structured oils. Figure 1 shows the changes on the oil body intrinsic proteins as a result of thermal treatment (heating and roasting). In Figure 1, L2 and L3 we can clearly see the three distinct bands of H-oleosin, L-oleosin, and caleosin in FOB, in addition to the strongly attached extraneous protease, P34/Bd30, and lipoxygenase (Chen, Chen, Zhao, Kong, Yang, & Hua, 2018). Upon roasting, the results agree well with our previous work on roasted peanut oil bodies (Zaaboul, et al., 2018; Zaaboul, Raza, Cao, & Yuanfa, 2019). All bands look like smears, broad bands at the top of the running gel and some bands look very intense, especially at 66, 37 and 20 KDa. It is notable that in Figure 1, L4, after heat treatment (heating), extraneous proteins were not observed indicating a release of such proteins. We also found that the intensity of the bands of the intrinsic proteins decreased, which was probably due to the heat treatment. It has been previously reported that heat treatment can affect and weaken the salt bridge between the two terminuses of oleosin and the phospholipid

membrane (Chen & Ono, 2010), and therefore could cause the release of this protein from its spatial position at the interface.

Based on the lipid and protein profile, we can clearly see that the only difference between the three oil bodies is the protein membrane composition resulting from the heat treatment (roasting and heating). We therefore probed any changes to the particle size of the oil bodies resulting from the change in the interfacial protein profile. Additionally, particle size of oil bodies in the mix is an extremely important parameter for a stable ice cream formulation. For example, a correlation between a small particle size and significantly better freezing has been observed, such as, favorable conditions leading to the creation of a smaller ice crystal structure and the retention of smaller ice crystals (Kot, Kamińska-Dwórznicka, & Jakubczyk, 2022). **Table 2** demonstrates that the three samples had different average particle sizes, with the largest observed for HOB and the smallest for the FOB. The increase in the size of the oil bodies after roasting the peanuts could be summarized mainly to a thickening protein coat. This agrees to changes in the oil body membrane proteins (Figure 1**)**, as for HOB, the increase in size is expected given the way oleosin is attached to the surface of oil bodies. According to Huang (Huang, 1992), the amino acid composition of the N- and C-termini of oleosin were characterized as containing more alkaline than acidic amino acids. These alkaline amino acids are attached to the negatively charged phospholipids *via* a salt bridge, which makes the two termini very close to oil bodies. However, it has been reported that the salt bridge can be transiently weakened by heating, causing the N- and C-termini to detach from the oil bodies (Chen & Ono, 2010). The electric charge is also an important parameter in any colloidal system. The zeta potential of the three oil body samples FOB, ROB and HOB was measured to be 25.75±0.35 mV, 28.8±0.85 mV and 26.4±0.4 mV, respectively (Table 2). A high value of zeta potential theoretically indicates high stability, while a low value of

zeta potential means low stability because a low repulsive force between droplets prevents them from flocculating and coming into close contact. After heating, the absolute value of zeta potential increased from 25.75 to 26.4 mV, which can be explained by the release of some positively charged extraneous proteins during heat treatment, but the two values were not statistically different. On the other hand, ROB showed a slightly higher zeta potential and was statistically different from FOB and HOB. We suggest that the change is due to the presence of new, negatively charged proteins on the surface of the oil bodies.

Table 2: Viscosity, flow behavior, consistency index, particle size of the Mix and OBs samples.

Samples	η	n	K	D_h of the Mix	D_h of OB	*Zeta potentiel*
	Pa·s			µm	µm	mV
FOB	75.74	0.72	16.51	0.92±0.04[a]	0.84±0.56[b]	25.75±0.35[a]
ROB	5.39	0.49	2.29	0.84±0.00[b]	1.03±0.02[c]	28.8±0.85[b]
HOB	4.08	0.56	3.84	1.26±0.06[c]	1.14±0.02[a]	26.4±0.4[ab]

Values are means ± Standard Deviation. Different letters within the same column are significantly different at $p < 0.05$. k: consistency index, n: flow behaviour index obtained from fitting experimental data to the Power law model and the η: apparent viscosity was calculated at shear rate of 100 s^{-1}. FOBs: Fresh oil bodies. ROBs: Roasted oil bodies, HOBs: Heat-treated oil bodies; OB: Oil bodies.

3.4 Rheological and micromechanical properties of ice cream mix

Upon probing the influence of oil bodies, viz., FOB, ROB, and HOB on the rheological and micromechanical properties of the formulated ice cream mix, we observed that all samples had indications of a Newtonian plateau suggestive of a pre-yielding viscosity. FOB showed the highest zero-shear viscosity corresponding to the plateau value of the complex viscosity, η^* (Figure 2 and Table 2), followed by decrease in ROB and HOB samples. All the samples exhibited a power law shear-thinning behaviour. The consistency coefficient (K) and flow behaviour (n) obtained using the power law model, for ice cream samples prepared with different oil bodies, are shown in Table

2. For a shear-thinning fluid, $0 < n < 1$. The shear-thinning nature of a system would increase as n tends towards zero. The flow behavior value of all samples ranged from 0.72 to 0.49, indicating that the ice cream mixes exhibit non-Newtonian pseudoplastic behavior. The consistency coefficient (K) is attributed to the colloidal particles in the ice cream mix (Damodaran, 1997). The results show that the nature of oil bodies can affect the consistency and flow of the mix, due to their particle size, proteins on the surface of oil bodies and interaction with other protein molecules in the system. The mix prepared with FOB had a high K value, while the mix prepared with HOB and ROB had the lower K value and they differ statically ($p < 0.05$). We postulate the difference in the consistency index of the three samples could be due to the differences in the intermolecular interactions, and these differences in the interactions were caused by changes in the composition of the FOB and ROB surface. The results are consistent with the altered protein composition of the oil bodies (as seen in Figure 1) after heat treatment and roasting of the beans and leads to a change in the intermolecular interactions between the oil bodies and the whey protein. Note, all results are within the linear viscoelastic range, and therefore would not lead to oil bodies deformation or sample breakage, as with steady-shear viscosity measurements.

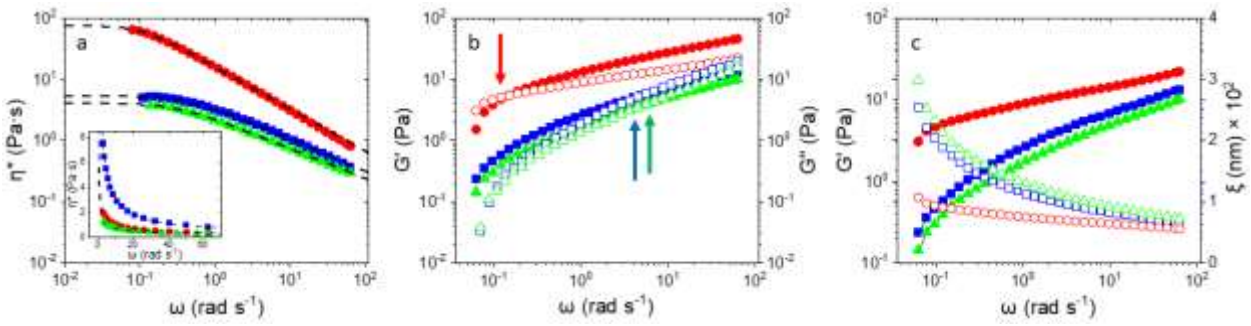

Figure 2. Complex viscosity (η^*) of ice cream mix versus angular frequency (ω) for FOB, ●; ROB, ■; HOB, ▲ at 4 °C. Carreau-Yasuda model function fits the data (dashed lines), where the coefficients of determination (R^2) were FOB, 0.99992; ROB, 0.99933; HOB, 0.99962. Inset shows non-logarithmic η^* versus high ω ; here, a Power-law model fits the data (dashed line) (a). Evolution of mean G' and G'' (FOB, ●; ROB, ■; HOB, ▲ at 4 °C) as a function of angular frequency. Arrows indicate the crossover point of G' and G'' (b). Evolution of mean G' (FOB, ●;

ROB, ■; HOB, ▲ at 4 °C) as a function of angular frequency and the average void volume (FOB, ● ; ROB, ■; HOB, ▲ at 4 °C) of ice cream mix (c). FOB: Fresh oil bodies. ROB: Roasted oil bodies, HOB: Heat treated oil bodies.

Additionally, we studied the frequency-wise kinetics of the ice cream mixtures to understand the micromechanical responses. From Figure 2b, the observed micromechanical responses reiterate our earlier observation of altered protein composition of the oil bodies. FOB samples tend to transition into the elastic regime much faster, compared to the ROB and HOB samples. The elastic modulus also provided us with information about the void volume in the samples. We evaluated the frequency-dependent data using the Maxwell model and by considering that an elastic energy equal to k_BT is stored within void volume ξ^3 in the samples (Borah, Yakubov, & Duary, 2021). Here, using a Gaussian repartition the relation becomes, $\xi = \sqrt[3]{(k_BT/G')}$, where k_B is the Boltzmann constant (1.38×10^{-23} m^2 kg s^{-2} K^{-1}) and T is the Kelvin temperature. Figure 2c shows the relationship between G' and void volume as a function of angular frequency. For example, the void volumes in FOB ranged from 107 nm to 55 nm with increasing frequency deformation. For ROB and HOB, the void volume change with frequency deformation was 300 nm to 72 nm and 250 nm to 70 nm, respectively. It is clear that the FOB system tends a reach a maximum fractional packing density even at lower frequency déformations, which explains the higher zero-shear viscosity and early transition into the elastic regime.

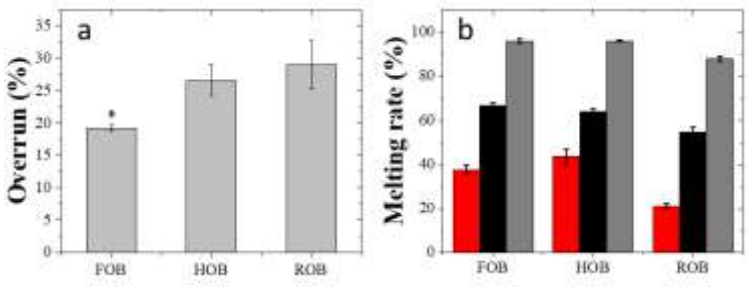

Figure 3. The overrun (a) and melting rate (b) of FOB, ROB, and HOB ice cream after 30-, 45-, and 60-min. Different letters indicate significant differences at $p < 0.05$. FOB: Fresh oil bodies. ROB: Roasted oil bodies, HOB: Heat-treated oil bodies.

3.5 Overrun and melting rate of ice cream. Since it was now evident that heating the oil bodies lead to dramatic differences in void volumes of the ice cream mixtures, as compared to oil bodies without heat modification, we first probed the overrun in the material which equates to the extent of air entrainment. Figure 3a shows the effect of roasting and heat treatment of peanut oil bodies on ice cream overrun. The use of treated oil bodies results in an increase in overrun from 18.95 ± 0.50 for FOB to 25.40 ± 2.41 for HOB and 27.19±3.77 for ROB. This difference clearly relates to lower void volumes in FOB, as compared to ROB and HOB, and we postulate is an effect of altered protein profile on the surface of oil bodies (*see protein profile*, Figure 1), as this was the only variable parameter in all mix samples. Modification of the oil body membrane resulted in changes in the particle size of oil bodies and the size of oil droplets in the mixes. ROB mix had the smallest particle size and highest overrun compared to FOB and HOB. It has been previously reported that reducing the particle size of oil droplets in the mix allows air to penetrate during freezing, which increases the overrun (Muzammil, Rasco, & Sablani, 2017). It was previously observed that the stability of oil bodies in peanut milk increases after roasting, and this improvement is primarily attributed to the presence of a second protein layer covering the oil bodies. Zaaboul et al., demonstrated that high-pressure homogenization followed by sterilization, resulted in the

366 destruction of all oil bodies in fresh peanut milk. This damage was evident through the separation
367 of the milk into two phases and the disappearance of oleosins, which serves as a marker for oil
368 body integrity. Interestingly, in contrast to fresh peanut milk, the stability of oil bodies in roasted
369 peanut milk remained unchanged even after undergoing the same processing treatments. This
370 indicates that the oil bodies in roasted peanut milk were protected by the second protein coat.
371 Building on this understanding, the current study explores the additional functions and properties
372 of the second protein layer. Besides providing protection against various stresses, this layer imparts
373 new functionalities to the oil bodies. Consequently, the oil bodies can interact with each other and
374 with the whey protein, resulting in the formation of a network that stabilizes air bubbles in the
375 peanut milk. The protein coating on the surface of oil bodies likely resulted in cross-linking with
376 the whey protein in the mix to form a stable steric structure that could prevent the collapse of the
377 air bubbles, leading to an increase in overrun (Kurt & Atalar, 2018). Although the viscosity of the
378 FOB mix was higher than that of the other samples, higher viscosity did not correlate with higher
379 overrun in our study, which is contrary to reports of previous studies. For example, Wang et. al.,
380 found a positive correlation between the increase in viscosity and the increase in overrun due to
381 the formation of stable and small air cells during the freezing process (Wang, Li, et al., 2022). The
382 viscosity is a measure of the resistance to the flow of the ice cream mix. On the other hand, the
383 overrun in ice cream refers to the increase in volume that occurs when air is incorporated into the
384 mixture and it is mainly related to the incorporation and stabilization of air bubbles in the ice
385 cream. The primary factor affecting air incorporation in ice cream is the ability of the ice cream
386 mix to entrap and stabilize air bubbles. This is primarily influenced by the structural properties of
387 the mix, such as the protein network. The viscosity alone does not necessarily determine the ability
388 of the mix to incorporate and stabilize air bubbles.

Additionally, upon probing the melting rate of the ice cream samples (Figure 3b). We observed that ROB significantly decreases the melting rate of ice cream at the 30th and 45th min while FOB and HOB melt at similar rates. At the 60th min, the melting rate of all samples was significantly the same, with ROB ice having the lowest value of 87.85 ± 1.18%, compared to 96 ± 1.01% and 96 ± 0.30% for FOB and HOB ice-creams, respectively. The final melting drop for each sample was at the 75th min for FOBs ice cream, at the 75th min for HOB ice cream, and at the 82nd min for the ROB ice cream. The noticeable decrease in overrun for ROB ice cream may be related to the fact that the overrun was higher, meaning that there were more air cells in the ice cream, which decreased the melting rate. Air is a poor conductor of heat, which decreases the heat diffusion rate of ice cream, thus decreasing the melting rate of ice cream. The particle size of the oil droplets in the mix may also play a role in reducing the melt rate by improving the stability of the ice cream emulsion system, thereby preventing the migration of water molecules, and reducing the melt rate of soybean oil bodies incorporated ice creams (Wang, Li, et al., 2022). We postulate that the main reason for ROB to have the ability to produce an ice cream with a higher overrun and a lower melting rate could be that the ROB tend to bridge with each other during the freezing and whipping process of the ice cream mix and form a continuous three-dimensional network, so that the air cells are enclosed and protected in this network during the freezing process, resulting in an increase in overrun and a decrease in melting rate. In contrast, the FOB and HOB ice creams with lower overrun and stability did not have enough spatial structure in the network to prevent melting and complete collapse.

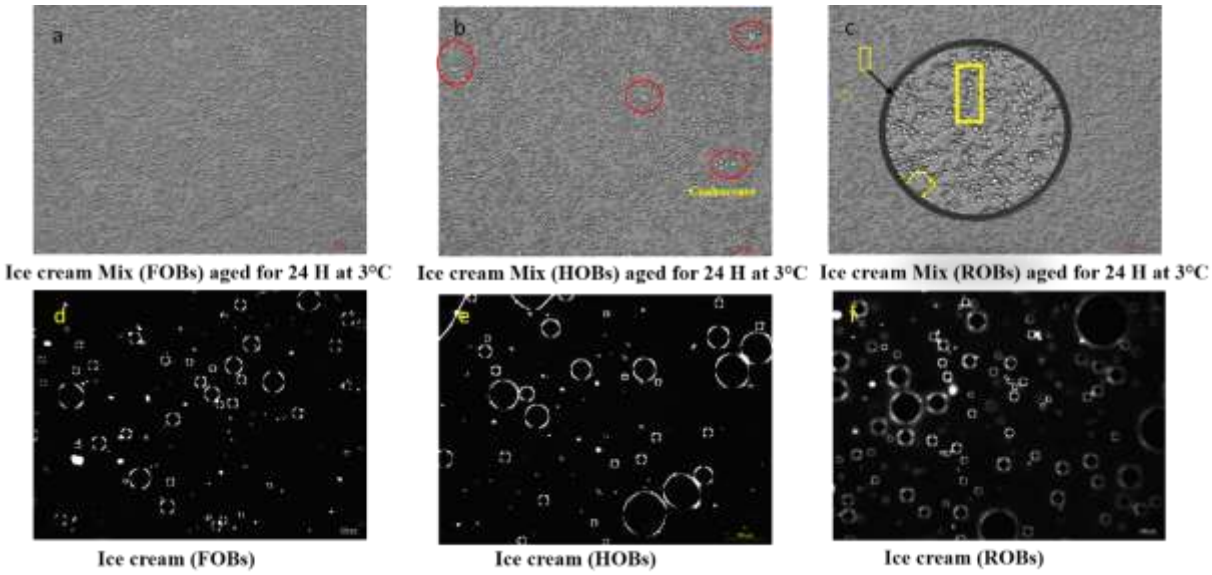

409

410 **Figure 4:** Microscopic visualization of the FOBs, ROBs and HOBs mixes, and the FOBs, ROBs
411 and HOBs ice creams. FOBs: Fresh oil bodies. ROBs: Roasted oil bodies, HOBs: Heat-treated oil
412 bodies.

413

414 To support our results, microscopic images of the mixes and the ice cream samples were
415 taken. In Figure 4, we see a clear difference in terms of the size of the lipid droplets and their
416 rearrangement. The FOB mix in Figure 4a shows a dense structure due to intense
417 aggregation/flocculation between the oil droplets and corroborates with our rheological and
418 micromechanical observations. The structure of the mix explains the low overrun due to this
419 compact structure. Figure 4d also shows that the FOB ice cream has few air cells due to the low
420 overrun, which explains the low resistance to ambient temperature during melting. The HOB mix
421 in Figure 4b shows that the oil bodies were arranged to form a random network with large oil
422 droplets, as a result of complete coalescence instead of partial coalescence, which we originally
423 aimed for. These results, in turn, explain why the HOB ice cream had a higher overrun than the
424 FOB mix, because the structure of the mix is less compact and forms a kind of network with
425 interstices that hold the air cells during the whipping and freezing process. Figure 4e shows why

the HOB mix has a higher overrun but a similar melting rate to the FOB mix. The air cells in the HOB ice cream were also few but larger, and due to the weak connection between the oil bodies in the HOB mix, the ice cream collapsed easily and showed similar melting resistance to the FOB ice cream. The microstructure of the ROB mix shows a better organized network with numerous small chambers of uniform oil bodies. It appears that the ROB form bridges among themselves without actually merging. This could be due to the formation of bonds between the second layer proteins on the ROB, which gave the same effect as the partial coalescence that normally occurs in the presence of animal-based fat. Figure 4f shows the presence of numerous air cells of different sizes, which is consistent with the structure of the mix in Figure 4c and the higher overrun and melting resistance compared to other samples. Overall, these results confirm the particle size, overrun and melting rate results of all samples.

3.8 Volatile components analysis. An important consideration of our study was to characterize flavor of the ice cream samples, based on modifications of the oil bodies. Flavor is one of the most important organoleptic properties of foods and the main reason why plant-based dairy products are not highly appreciated by consumers due to their grassy and beany taste. One of the reasons why we decided to roast the peanuts before extracting the oil bodies was to remove the beany flavor and preserve the nuttiness of the Maillard reaction. We also heated the fresh oil bodies for 15 min to denature the oxygenase and lipoxygenase responsible for the beany flavor as a result of oxidation of the polyunsaturated fatty acids (Laswai, Thonya, Yesaya, Silayo, Kulwa, Mpagalile, et al., 2009). Supplementary Information Figure S2 shows the main volatiles found in the three ice cream samples containing FOB, HOB and ROB as fat replacers. In the FOB ice cream, the volatiles responsible for the green and beany flavor, such as *n*-hexanal and 2-pentenylfuran, had the highest proportion, together accounting for ca. 71%. Trans-2-heptenal was the second most abundant

449 volatile after *n*-hexanal. It is known for its sweet flavor (Maul, Sargent, Sims, Baldwin, Balaban,
450 & Huber, 2000); however, previous studies have reported that a strong greasy, fatty taste is always
451 associated with the presence of trans-2-heptenal (Feng, Hua, Li, Zhang, Kong, & Chen, 2020).
452 After heat treatment of the FOB, the volatile profile of the ice cream changed. Some new volatiles
453 appeared, and others disappeared. For example, *n*-hexanal decreased significantly and new
454 volatiles responsible for the green, beany flavor appeared, such as 3-hexen-1-ol and 1,3,8-p-
455 menthatriene, the key flavor component of parsley leaves (Masanetz & Grosch, 1998). Other
456 aromas such as isosaphrone also occur in high concentrations. This aroma is characteristic of
457 saffron and is produced by the thermal degradation of trans-crocetin esters (Cid-Pérez, Nevárez-
458 Moorillón, Ochoa-Velasco, Navarro-Cruz, Hernández-Carranza, & Avila-Sosa, 2021). After
459 roasting, we expected an abundance of volatiles characteristic of the nutty flavor, such as pyrazine
460 compounds (Leunissen, Davidson, & Kakuda, 1996; Yin, Maradza, Xu, Ma, Shi, Zhao, et al.,
461 2022), but 2-acetyl-1-pyrroline was the only component detected and at low concentration. This
462 low content could be since all the flavors included in the oil bodies were not released during the
463 SPME analysis. On the other hand, new components previously reported in roasted peanuts and
464 peanut oils were detected, including 1-hexanol (green flavor), which appeared for the first time in
465 a roasted sample, and these results are consistent with previous work on roasted peanuts. Leunissen
466 et al. found that mild roasting caused an increase in 1-hexanol in roasted peanuts (Leunissen,
467 Davidson, & Kakuda, 1996). Nonanal (floral flavor), is a characteristic aroma of peanut oil (Zhang,
468 He, Zhang, Li, Jin, Liu, et al., 2022), 1-octen-3-ol (metallic beany flavor) was previously detected
469 in roasted peanuts (Asikin, Tanahara, Maeda, Tsuchida, Hirose, Oe, et al., 2021). Fruity flavors
470 were also detected in ROB ice cream, such as *D*-limonene (fruity flavor) (Liu, Jin, Liu, Huang,
471 Wang, Mao, et al., 2011), Butyl butyrate (fruity flavor) and methyl cinnamate (strawberry flavor)

(Schirack, Drake, Sanders, & Sandeep, 2006) all these volatiles were previously reported to be found in roasted peanuts. Heat treatment and roasting did noticeably change the volatile profile of oil body incorporated ice cream due to the attachment of these flavors for the oil bodies, however, sensory evaluation is still needed to evaluate the actual taste of the ice cream and whether more nuttiness would be release while consuming the ice cream, which is beyond the scope of the current study.

Conclusion. It is concluded that incorporation of heat treatment of oil bodies as a fat replacer in ice cream, progressively alters the intrinsic protein profile of oil bodies, which results in marked differences in rheological and micromechanical responses, as well as physical properties of ice cream. Our results show that the protein membrane of peanut oil bodies (heated oil bodies) has a great influence on how oil bodies react with other ice cream ingredients, leading to the formation of ice cream with different properties. Heat treatment and roasting altered the protein membrane of oil bodies. Roasting leads to the formation of a second protein layer over the intrinsic protein layer, while heat treatment removes most of the endogenous proteins and leaves the oil bodies with a very thin membrane that would favor partial coalescence, but microscopic visualization showed us complete coalescence instead of partial coalescence. These changes were responsible for the large changes in the physicochemical properties of the ice cream. The results showed that the viscosity of FOB (fresh oil bodies) was greater compared to ROB (roasted oil bodies) and HOB. The consistency index decreased, and the flow behavior increased (*i.e.*, pseudoplasticity) for ROB and HOB. The overrun level and melting rate of the ice cream samples were also affected using ROB in the preparation of ice cream. This positive effect was explained by microscopic visualization of the mix and ice cream samples. The volatiles responsible for the grassy and beany flavor of the FOB decreased significantly after roasting and heat treatment. However, it seems that

the oil bodies did not fully release the flavor packed in them, as we could not detect many notes indicating a nutty flavor. Overall, based on these preliminary results, the present work sets the foundation for future research to develop the peanut oil bodies as a fat substitute for developing plant-based ice creams.

Authorship contribution statement

FZ: Investigation, Conceptualization, Methodology, Software, Data curation, Formal analysis, Writing- Original draft preparation; TT: Data curation; PKB: Writing- Reviewing and Editing.; VDB: Writing- Reviewing and Editing.

Declaration of Competing Interest

The authors declare that they have no known competing financial interest or personal relationships that could have appeared to influence the work reported in this paper.

Acknowledgement

This work was supported by National Natural Science Foundation of China (Grant No 311500410375)

References:

Akalin, A., & Karagzl, C. nal G (2008) Rheological properties of reduced-fat and low fat ice cream containing whey protein isolate and inulin. *Eur Food Res Technol*, *227*(3), 889895.

Akbari, M., Eskandari, M. H., & Davoudi, Z. (2019). Application and functions of fat replacers in low-fat ice cream: A review. *Trends in Food Science & Technology*, *86*, 34-40.

Asikin, Y., Tanahara, N., Maeda, G., Tsuchida, E., Hirose, N., Oe, M., Takara, K., & Wada, K. (2021). Odorous volatiles and methoxypyrazines responsible for the musty-peanut aroma in microwave-heated sponge gourd (*Luffa cylindrica*). *Food Science and Technology Research*, *27*(6), 933-938.

Bekiroglu, H., Goktas, H., Karaibrahim, D., Bozkurt, F., & Sagdic, O. (2022). Determination of rheological, melting and sensorial properties and volatile compounds of vegan ice cream produced with fresh and dried walnut milk. *International Journal of Gastronomy and Food Science*, *28*, 100521.

Borah, P. K., Yakubov, G. E., & Duary, R. K. (2021). Rheology, microstructure and diffusion in soft gelatin nanocomposites packed with anionic nanogels. Food Structure, 30, 100216. https://doi.org/https://doi.org/10.1016/j.foostr.2021.100216.

Chen, Y., & Ono, T. (2010). Simple extraction method of non-allergenic intact soybean oil bodies that are thermally stable in an aqueous medium. *Journal of agricultural and food chemistry*, *58*(12), 7402-7407.

Chen, Y., Chen, Y., Zhao, L., Kong, X., Yang, Z., & Hua, Y. (2018). A two-chain aspartic protease present in seeds with high affinity for peanut oil bodies. Food chemistry, 241, 443-451.

Cid-Pérez, T. S., Nevárez-Moorillón, G. V., Ochoa-Velasco, C. E., Navarro-Cruz, A. R., Hernández-Carranza, P., & Avila-Sosa, R. (2021). The relation between drying conditions

534 and the development of volatile compounds in saffron (*Crocus sativus*). *Molecules*, *26*(22),
535 6954.
536 Crizel, T. d. M., Araujo, R. R. d., Rios, A. d. O., Rech, R., & Flôres, S. H. (2014). Orange fiber as
537 a novel fat replacer in lemon ice cream. *Food Science and Technology*, *34*, 332-340.
538 Damodaran, S. and Paraf, A. (1997). Food proteins and their applications. Marcel Dekker, Inc.,
539 New York.
540 Diaby, M., Amza, T., Onivogui, G., Zou, X., & Jin, Q. (2016). Physicochemical and antioxidant
541 characteristics of gingerbread plum (*Neocarya macrophylla*) kernel oils. *Grasas y Aceites*,
542 *67*(1), e117-e117.
543 Feng, X., Hua, Y., Li, X., Zhang, C., Kong, X., & Chen, Y. (2020). (E)-2-Heptenal in soymilk: A
544 Nonenzymatic Formation Route and the Impact on the Flavor Profile. *Journal of agricultural*
545 *and food chemistry*, *68*(50), 14961-14969.
546 Goff, H. D., & Hartel, R. W. (2013). Composition and Formulations. In H. D. Goff & R. W. Hartel
547 (Eds.), Ice Cream, (pp. 19-44). Boston, MA: Springer US.Huang, A. H. (1992). Oil bodies
548 and oleosins in seeds. *Annual review of plant biology*, *43*(1), 177-200.
549 Jiang, J., Jin, Y., Liang, X., Piatko, M., Campbell, S., Lo, S. K., & Liu, Y. (2018). Synergetic
550 interfacial adsorption of protein and low-molecular-weight emulsifiers in aerated
551 emulsions. *Food Hydrocolloids*, *81*, 15-22.
552 Kot, A., Kamińska-Dwórznicka, A., & Jakubczyk, E. (2022). Study on the influence of ultrasound
553 homogenisation on the physical properties of vegan ice cream mixes. *Applied Sciences*,
554 *12*(17), 8492.
555 Kurt, A., & Atalar, I. (2018). Effects of quince seed on the rheological, structural and sensory
556 characteristics of ice cream. *Food Hydrocolloids*, *82*, 186-195.

557 Laswai, H. S., Thonya, N., Yesaya, D., Silayo, V., Kulwa, K., Mpagalile, J., & Ballegu, W. (2009).
558 Use of locally available flavouring materials in suppressing the beany taste in soymilk.
559 *African Journal of Food, Agriculture, Nutrition and Development*, *9*(7).
560 Leunissen, M., Davidson, V. J., & Kakuda, Y. (1996). Analysis of volatile flavor components in
561 roasted peanuts using supercritical fluid extraction and gas chromatography−mass
562 spectrometry. *Journal of Agricultural and Food Chemistry*, *44*(9), 2694-2699.
563 Liu, X., Jin, Q., Liu, Y., Huang, J., Wang, X., Mao, W., & Wang, S. (2011). Changes in volatile
564 compounds of peanut oil during the roasting process for production of aromatic roasted
565 peanut oil. *Journal of food science*, *76*(3), C404-C412.
566 Mao, B., Guo, W., Huang, Z., Tang, X., Zhang, Q., Yang, B., Zhao, J., Cui, S., & Zhang, H. (2022).
567 Production of conjugated fatty acids in probiotic-fermented walnut milk with the addition
568 of lipase. LWT, 172, 114204.
569 Marshall, R. T., Goff, H. D., Hartel, R. W., Marshall, R. T., Goff, H. D., & Hartel, R. W. (2003).
570 Ice cream ingredients. *Ice cream*, 55-87.
571 Masanetz, C., & Grosch, W. (1998). Key odorants of parsley leaves (*Petroselinum crispum* [Mill.]
572 *Nym. ssp. crispum*) by Odour–activity values. *Flavour and fragrance journal*, *13*(2), 115-
573 124.
574 Maul, F., Sargent, S., Sims, C., Baldwin, E., Balaban, M., & Huber, D. (2000). Tomato flavor and
575 aroma quality as affected by storage temperature. *Journal of food science*, *65*(7), 1228-
576 1237.
577 Muzammil, H. S., Rasco, B., & Sablani, S. (2017). Effect of inulin and glycerol supplementation
578 on physicochemical properties of probiotic frozen yogurt. *Food & nutrition research*,
579 *61*(1), 1290314.

580 Schirack, A. V., Drake, M. A., Sanders, T. H., & Sandeep, K. P. (2006). Characterization of aroma-
581 active compounds in microwave blanched peanuts. *Journal of food science, 71*(9), C513-
582 C520.
583 Sempore, G., & Bezard, J. (1986). Qualitative and quantitative analysis of peanut oil
584 triacylglycerolsby reversed-phase liquid chromatography. *Journal of Chromatography A,*
585 *366*, 261-282.
586 Singleton, J., & Pattee, H. (1987). Characterization of peanut oil tricacyglycerols by HPLC, GLC
587 and EIMS. *Journal of the American Oil Chemists Society*, *64*(4), 534-538.
588 Sun, F., Wang, Q., Gao, C., Xiao, H., & Yang, N. (2023). Effect of extraction pH and post-
589 extraction heat treatment on the composition and interfacial properties of peanut oil bodies.
590 Colloids and Surfaces A: Physicochemical and Engineering Aspects, 656, 130351.
591 VanWees, S. R., Rankin, S. A., & Hartel, R. W. (2020). The microstructural, melting, rheological,
592 and sensorial properties of high-overrun frozen desserts. *J Texture Stud*, *51*(1), 92-100.
593 Wang, W., Li, J., Wang, M., Gu, L., Liu, Z., Xu, C., Ma, J., Jiang, L., Jiang, Z., & Hou, J. (2022).
594 Soybean-oil-body-substituted low-fat ice cream with different homogenization pressure,
595 pasteurization condition, and process sequence: physicochemical properties, texture, and
596 storage stability. *Foods, 11*(17), 2560.
597 Wang, F. C., Gravelle, A. J., Blake, A. I., & Marangoni, A. G. (2016). Novel trans fat
598 replacement strategies. Current Opinion in Food Science, 7, 27-34.
599 Wang, W., Wang, M., Xu, C., Liu, Z., Gu, L., Ma, J., Jiang, L., Jiang, Z., & Hou, J. (2022). Effects
600 of soybean oil body as a milk fat substitute on ice cream: Physicochemical, sensory and
601 digestive properties. *Foods, 11*(10), 1504.

602 Yin, W.-t., Maradza, W., Xu, Y.-f., Ma, X.-t., Shi, R., Zhao, R.-y., & Wang, X.-d. (2022).
603 Comparison of key aroma-active composition and aroma perception of cold-pressed and
604 roasted peanut oils. *International Journal of Food Science & Technology, 57*(5), 2968-
605 2979.
606 Zaaboul, F., Cao, C., Raza, H., Jun, Z. Z., Xu, Y. J., & Liu, Y. F. (2019). The triacylglycerol profile
607 of oil bodies and oil extracted from argania spinosa using the uplc along with the
608 electrospray ionization quadrupole-time-of-flight mass spectrometry (LC-Q-TOF-MS).
609 *Journal of food science, 84*(4), 762-769.
610 Zaaboul, F., Matabaro, E., Raza, H., Xin, B. D., Duhoranimana, E., Cao, C., & Liu, Y. (2018).
611 Validation of a simple extraction method for oil bodies isolated from peanuts. *European*
612 *Journal of Lipid Science and Technology, 120*(2), 1700363.
613 Zaaboul, F., Raza, H., Cao, C., & Yuanfa, L. (2019). The impact of roasting, high pressure
614 homogenization and sterilization on peanut milk and its oil bodies. *Food chemistry, 280*,
615 270-277.
616 Zaaboul, F., Raza, H., Chen, C., & Liu, Y. (2018). Characterization of peanut oil bodies integral
617 proteins, lipids, and their associated phytochemicals. *Journal of food science, 83*(1), 93-
618 100.
619 zaaboul, F., Zhao, Q., Xu, Y., & Liu, Y. (2022). Soybean oil bodies: A review on composition,
620 properties, food applications, and future research aspects. *Food Hydrocolloids, 124*,
621 107296.
622 Zhang, Z., He, S., Zhang, L., Li, X., Jin, R., Liu, Q., Chen, S., Wang, J., & Sun, H. (2022). The
623 potential application of vegetable oils in the D-xylose and L-cysteine Maillard reaction
624 system for meaty aroma production. *Food Research International, 155*, 111081.